

Stem Cell Reports, Volume 17

Supplemental Information

Directly induced human retinal ganglion cells mimic fetal RGCs and are neuroprotective after transplantation *in vivo*

Ziming Luo, Kun-Che Chang, Suqian Wu, Catalina Sun, Xin Xia, Michael Nahmou, Minjuan Bian, Rain R. Wen, Ying Zhu, Sahil Shah, Bogdan Tanasa, Marius Wernig, and Jeffrey L. Goldberg

Supplementary method:

1. Primary RGC culture and lentivirus construction

RGCs from P2 mice were purified and cultured as published (Trakhtenberg et al., 2014). Briefly, whole retinas were dissected and dissociated with papain, and subsequently were immunopanned with the Thy1 antibody. Purified RGCs were plated on poly-D-lysine- and laminin-coated coverslips and cultured for 3-4 days in RGC culture medium (describe below) before calcium imaging.

Plasmids of lentivirus (rtTA, NGN2, and EGFP) were generated as previously published (Zhang et al., 2013). Lentiviruses (rtTA, NGN2, and EGFP, 10^8 TU/ml) were produced by Stanford Gene and Virus Core, and AAVnerGene, Inc. LV-CMV-Cre-GFP-puro lentivirus was purchased from SignaGen Laboratories.

2. Generation of iRGCs from human ESCs and iPSCs

hESCs and hiPSCs were treated with 0.5% EDTA and plated on Matrigel (BD Biosciences)-coated plates at 70% confluence in StemFlex (Thermo Fisher Scientific) on day -2. On day -1, lentivirus prepared as previously described (Zhang *et al.*, 2013) was added in fresh StemFlex medium. On day 0, the culture medium was replaced with NBF (1% B27 supplement, 0.5% N2 supplement, 20 ng/ml fibroblast growth factor and 1% penicillin/streptomycin in DMEM-F12 medium). Doxycycline (2 μ g/ml, Clontech) was added on day 0 to induce TetO expression. On day 1, 2 μ g/ml puromycin was added in fresh NBF medium for a 24 hr selection. On day 2, the culture medium was replaced with RGC culture medium (Full Sato, prepared as previously described (Wu et al., 2018)), including insulin (5 μ g/ml, Sigma), sodium pyruvate (1 mM, Sigma), penicillin/streptomycin (1%, Thermo Fisher Scientific), Sato supplement (1:100), L-glutamine (1 mM, Sigma), triiodothyronine (T3, 40 ng/ml, Sigma), *N*-acetyl cysteine (5 μ g/ml, Sigma), brain-derived neurotrophic factor (50 ng/ml, Peprotech), ciliary neurotrophic factor (10 ng/ml, Peprotech), forskolin (5 mM, Sigma) (Barres et al., 1988) plus Notch inhibitor DAPT (10 μ M, EMD Millipore) and glial derived neurotrophic factor (50 μ g/ml, Peprotech) for another 4 days, changing half of the medium every other day.

3. Quantitative real-time PCR

Total RNA was isolated from retinal tissue or cells in culture according to the manufacturer's

protocol (RNeasy Microarray Tissue Mini Kit, Qiagen). RNA (5 µg) was reverse transcribed using iScript™ cDNA Synthesis Kit (Bio-Rad). For qRT-PCR, the iTaq™ Universal SYBR® Green Supermix (Bio-Rad) was used according to the manufacturer's protocol on a CFX Connect™ Real-Time PCR Detection System (Bio-Rad). Taqman primers for human *GAPDH*, *OCT4*, *NANOG*, *PAX6*, *POU4F1*, and *ISL1* were directly purchased from Thermo Fisher Scientific (Waltham, MA USA). The thermocycler parameters were 94 °C for 5 min, followed by 40 cycles of 94 °C for 30 sec, 56 °C for 30 sec and 72 °C for 60 sec. For the qPCR in Fig. 1, the LightCycler480 SYBR Green I Master (4887352001-1; Roche, Basel Switzerland) was used according to the manufacturer's protocol. Primers for human *GAPDH* (forward: GTCTCCTCTGACTTCAACAGCG, reverse: ACCACCCTGTTGCTGTAGCCAA), *ATOH7* (forward: GGTCTCCACTGTGAGCACTTCG, reverse: TGG AAGCCGAAGAGTCTCTGGC), *DLL3* (forward: CACTCAACAACCTAAGGACGCAG, reverse: GAGCGTAGATGGAAGGAGCAGA), and *HES6* (forward: GCTGGAGAACGCCGAAGTGCT, reverse: TGGACACGAACGTGTGCACCTC) were synthesis by Genewiz (South Plainfield, NJ, USA). *GADPH* was used as internal control. All qRT-PCR data was analyzed by $2\Delta Ct$. All experiments were repeated at least three times for statistical comparison.

4. Immunostaining

Cells cultured on coated glass slides or dishes were fixed with warm 4% PFA at room temperature for 20 min and then washed with PBS three times. After permeabilizing with 0.1% Triton X-100, cells were blocked with 10% BSA and incubated with primary antibodies including mouse anti-Brn3a antibody (1:50, Millipore, MAB1585), rabbit anti-Tuj1 (1:300, Cell Signaling Technology, CST5568), rabbit anti-Islet1 (1:250, Abcam, Ab109517), mouse anti-CHX10 (1:20, Santa Cruz Technology, sc374151), mouse anti-NEFL (1:50, Santa Cruz Technology, sc20012) and rabbit anti-Ki67 (1:200, Abcam, Ab115580) overnight at 4 °C. Alexa-488, Alexa-546, and Alexa-647 (Thermo Fisher Scientific) fluorescent antibodies were used for secondary detection. DAPI (Life Technologies) was used for nuclei staining.

Eye globes of transplanted mice were fixed with 4% PFA overnight, followed by 15% and 30% sucrose overnight. Cryo-sectioning was performed, and the 10 µm sections were incubated with

guinea pig anti-RBPMS (gift from Dr. Yang Hu, Stanford Ophthalmology) and mouse anti-human nuclear antigen antibody (1:200, Abcam, Ab191181) overnight at 4 °C in humidity chamber. Goat Alexa-488 antibody (Thermo Fisher Scientific) and DAPI were used for fluorescence and nuclei detection, respectively. All images were taken using fluorescence microscopy (Zeiss) or confocal microscopy (LSM 880, Zeiss).

5. Calcium imaging

Coverslips with cultured cells were incubated for 30 min at room temperature with 4 μ M Fluo 4-AM (Invitrogen, F14201) in Tyrode's solution (pH 7.4): NaCl 129 mM, KCl 5 mM, CaCl₂ 2 mM, MgCl₂ 1 mM, glucose 30 mM and HEPES 25 mM, containing 1 mg/ml bovine serum albumin. After washing with 'Tyrode's solution, the cells were placed in an imaging chamber (RC-26GLP, Warner Instruments) and perfused with 'Tyrode's solution while imaging. Calcium imaging was performed on an inverted fluorescence microscope (AxioObserver, Zeiss) with a fast-switching light source (DG-4, Sutter Instruments) using MetaFluor software (Molecular Devices) working within a linear range of the camera. Regions of interest (ROIs) were drawn around labeled cell bodies corresponding to cells with a neuronal morphology. As a control, in each field of view, 1-2 ROIs were also drawn around cells with non-neuronal, glia-like morphology. Calcium responses within ROIs were observed as changes in the fluorescence ratio (340/380) upon sequential stimulation with muscimol (100 μ M, Sigma-Aldrich, M1523) and KCl (30 mM). Each point on the summary plots corresponds to the fraction of cells in each experiment that responded to muscimol. KCl was used as a positive stimulus for neuronal cells, and 100% of the cells responded to KCl in the present experiments.

6. Cell dissociation for deep sequencing

iRGCs were dissociated using Accutase (Innovative Cell Technologies) for 15-20 minutes on day 6. Cell pellets were resuspended in PBS containing 0.04% bovine serum albumin and filtered through a 40 μ m cell strainer (Falcon, Cat#352340) to remove cell clumps before counting with a hemocytometer. Barcoded 3' single-cell libraries were prepared from single cell suspensions using the Chromium Single Cell 3' Library and Gel Bead kit (10X Genomics, Pleasanton, California) for sequencing according to the recommendations of the manufacturer. The cDNA and library fragment size distribution were verified via micro-capillary gel electrophoresis on a Bioanalyzer

2100 (Agilent, Santa Clara, CA). The libraries were quantified by fluorometry on a Qubit instrument (LifeTechnologies, Carlsbad, CA) and by qPCR with a Kapa Library Quant kit (Kapa Biosystems-Roche) prior to sequencing. Eight libraries were sequenced per lane on a NovaSeq 6000 sequencer (Illumina, San Diego, CA) with paired-end 150 bp reads.

7. scRNA-seq analysis

7.1 Data processing

We applied fastp with the default parameters filtering the adaptor sequence, and removed the low-quality reads to achieve clean data. Then the feature-barcode matrices were obtained by aligning reads to the human genome using CellRanger v3.0.0. Seurat analysis was performed in R using Seurat (v3.2.0), ggplot2, dplyr. The data were normalized by log normalization and scaled, and PCs were computed. Cell clustering was visualized by tSNE dimensional reduction in Figure 3. For Figure 4 and Figure 5 A-B, different time points of fetal retina (Day-59 and -82) and retinal organoid (Day-60 and -82) datasets were integrated, respectively, by identifying "anchors" across single-cell datasets (Stuart et al., 2019). Subsequently, iRGCs (clusters 3 and 4) were extracted as subsets from the Figure 3 dataset. iRGC data were then integrated with a fetal dataset or retinal organoid dataset. Cell clustering was visualized by UMAP dimensional reduction. For Figure 5C, RGCs in day-45 retinal organoids were identified by *SNCG*, *GAP43*, and *NEFL* and extracted. Then, we integrated the iRGC data and day-45 retinal organoid-derived RGC data and performed UMAP dimensional reduction. For Figure 6, the whole rapid protocol differentiation dataset was integrated with a Day-5 iN dataset or Day-93 cortical organoid dataset (Fair et al., 2020).

7.2 Pseudotime analyses

We applied the single-cell Trajectory analysis utilizing Monocle2 with default parameters. We perform a completely "unsupervised" analysis for the machine learning approach. Then, we reduced dimensions by DDR Tree and ordered cells in pseudotime. By using the function "plot_genes_branched_pseudotime", we plotted *SOX4* and *SOX11* to show the different kinetic trends for each lineage along pseudotime.

7.3 Gene ontology (GO) analyses

The GO analyses were performed on Enrichr (<https://maayanlab.cloud/Enrichr/>) (Chen et al., 2013; Kuleshov et al., 2016). The top 5 GO annotations are shown in the present data.

8. Animals for cell transplant

All animal research was conducted in compliance with ARVO statement for the use of animals in ophthalmic and vision research and was approved by Institutional Animal Care and Use Committee at Stanford University. C57BL/6 wild-type (WT) male and female mice at 4 to 6 weeks old and Sprague Dawley female rats at 6 weeks old were obtained from Charles River. 10^4 and 10^5 differentiated cells were intravitreally injected to mice and rats, respectively. Optic nerve crush (ONC) was conducted on 6~8-week old male mice as previously described (Cameron et al., 2020). iRGC were injected either immediately or 1 month after ONC, and the retinas were collected 1 week or 1 month after transplant. Endogenous RGCs were stained by RBPMS and counted manually following the previously published protocol (Cameron *et al.*, 2020). Cre-driven tdTomato mice were obtained from The Jackson Laboratory. In some cases, control (no ONC) donor cell engraftment failed altogether; merging control groups across experiments was used to facilitate comparisons.

9. Statistical analysis

Results are shown as the Means \pm SEM of at least three experiments. Data were analyzed by ANOVA with Tukey's test and paired t-test with a *P*-value of <0.05 considered significant.

References:

- Barres, B.A., Silverstein, B.E., Corey, D.P., and Chun, L.L. (1988). Immunological, morphological, and electrophysiological variation among retinal ganglion cells purified by panning. *Neuron* *1*, 791-803.
- Cameron, E.G., Xia, X., Galvao, J., Ashouri, M., Kapiloff, M.S., and Goldberg, J.L. (2020). Optic Nerve Crush in Mice to Study Retinal Ganglion Cell Survival and Regeneration. *Bio Protoc* *10*. 10.21769/BioProtoc.3559.
- Chen, E.Y., Tan, C.M., Kou, Y., Duan, Q., Wang, Z., Meirelles, G.V., Clark, N.R., and Ma'ayan, A. (2013). Enrichr: interactive and collaborative HTML5 gene list enrichment analysis tool. *BMC Bioinformatics* *14*, 128. 10.1186/1471-2105-14-128.
- Fair, S.R., Julian, D., Hartlaub, A.M., Pusuluri, S.T., Malik, G., Summerfield, T.L., Zhao, G., Hester, A.B., Ackerman, W.E.t., Hollingsworth, E.W., et al. (2020). Electrophysiological Maturation of Cerebral Organoids Correlates with Dynamic Morphological and Cellular Development. *Stem Cell Reports* *15*, 855-868. 10.1016/j.stemcr.2020.08.017.
- Kuleshov, M.V., Jones, M.R., Rouillard, A.D., Fernandez, N.F., Duan, Q., Wang, Z., Koplev, S., Jenkins, S.L., Jagodnik, K.M., Lachmann, A., et al. (2016). Enrichr: a comprehensive gene set enrichment analysis web server 2016 update. *Nucleic Acids Res* *44*, W90-97. 10.1093/nar/gkw377.
- Stuart, T., Butler, A., Hoffman, P., Hafemeister, C., Papalexi, E., Mauck, W.M., 3rd, Hao, Y., Stoeckius, M., Smibert, P., and Satija, R. (2019). Comprehensive Integration of Single-Cell Data. *Cell* *177*, 1888-1902 e1821. 10.1016/j.cell.2019.05.031.
- Trakhtenberg, E.F., Wang, Y., Morkin, M.I., Fernandez, S.G., Mlacker, G.M., Shechter, J.M., Liu, X., Patel, K.H., Lapins, A., Yang, S., et al. (2014). Regulating Set-beta's Subcellular Localization Toggles Its Function between Inhibiting and Promoting Axon Growth and Regeneration. *The Journal of neuroscience : the official journal of the Society for Neuroscience* *34*, 7361-7374. 10.1523/JNEUROSCI.3658-13.2014.
- Wu, S., Chang, K.C., Nahmou, M., and Goldberg, J.L. (2018). Induced Pluripotent Stem Cells Promote Retinal Ganglion Cell Survival After Transplant. *Invest Ophthalmol Vis Sci* *59*, 1571-1576. 10.1167/iovs.17-23648.
- Zhang, Y., Pak, C., Han, Y., Ahlenius, H., Zhang, Z., Chanda, S., Marro, S., Patzke, C., Acuna, C., Covy, J., et al. (2013). Rapid single-step induction of functional neurons from human pluripotent stem cells. *Neuron* *78*, 785-798. 10.1016/j.neuron.2013.05.029.

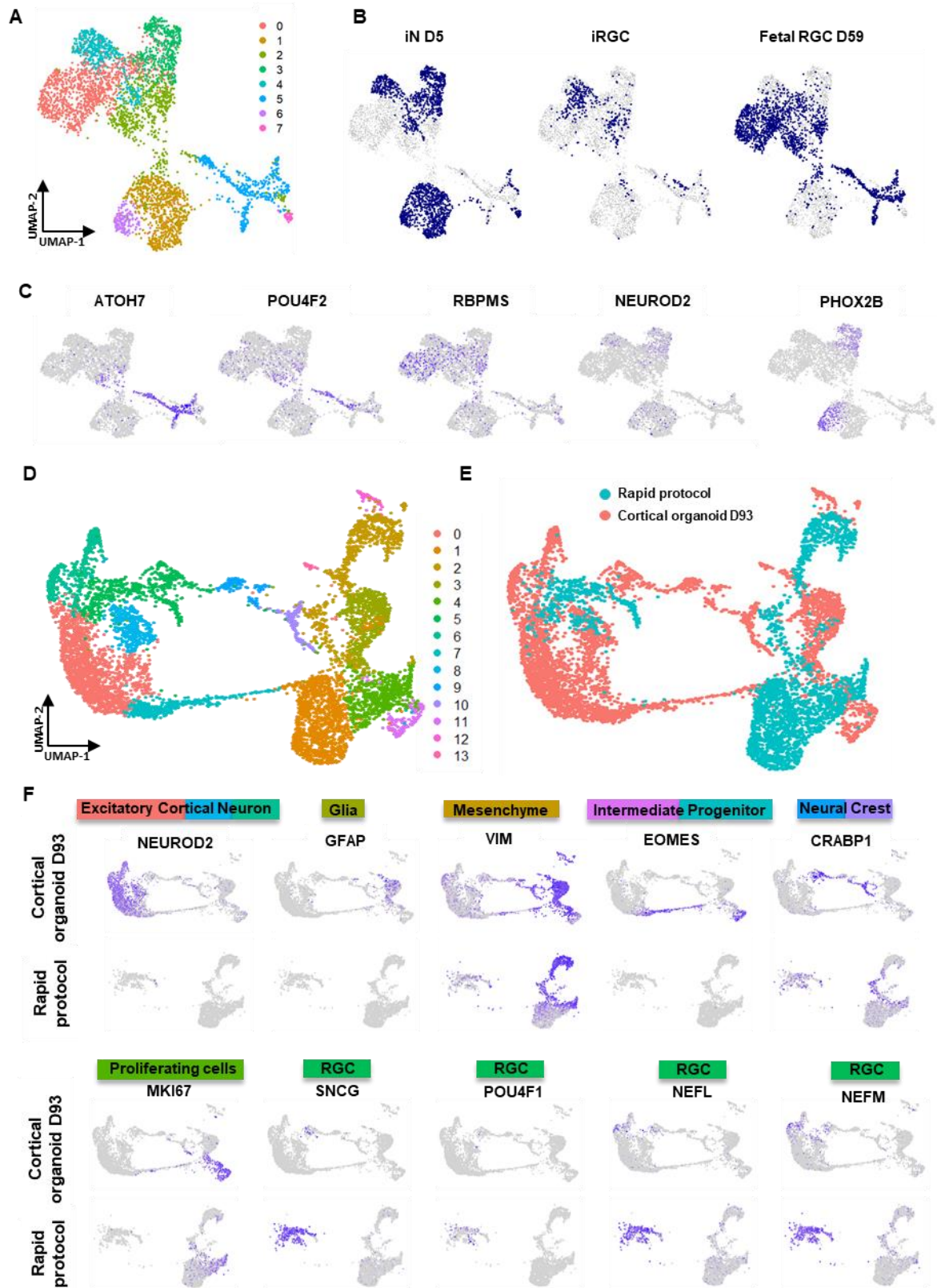


Figure. S1. Rapid protocol-derived iRGCs are transcriptionally different from iNs and from cortical organoid cell progeny. (A) Combined UMAP plot showing iRGCs, D59 fetal RGCs, and iNs derived from the original protocol. (B) UMAP plotted by tissue of origin demonstrates overlap of iRGC with subsets of fetal RGCs, but iN progeny are largely distinct from fetal RGCs, particularly in clusters 1, 3 and 6. (C) Feature plots show that iRGCs express RGC markers, but not the cortical neuron marker, *NEUROD2*, nor the rhombencephalon/brain stem marker, *PHOX2B*, which is expressed in iN progeny. (D) Combined UMAP plot of D93 cortical organoid and rapid protocol-derived cells. (E) UMAP plot showing the tissues of origin demonstrates that many clusters (from A) contain cells of each differentiation protocol, although the iRGCs are largely segregated from the cortical organoid cells in each case. (F) Feature plots of cortical cell type genes and RGC-specific genes in the combined dataset (labeled above each plot) demonstrate that among neuronal clusters 0, 6, and 7, RGCs make up a distinct subset largely absent from cortical organoid differentiation. Conversely, cortical organoid-derived intermediate progenitors and other progeny are largely absent in rapid-protocol iRGC differentiation. Plots were split by tissue of origin.